A local glutamate-glutamine cycle sustains synaptic excitatory transmitter release

Hiroaki Tani[1,*], **Chris G. Dulla**[2], **Zoya Farzampour**[1,3], **Amaro Taylor-Weiner**[2], **John R. Huguenard**[1,3], and **Richard J. Reimer**[1,3,4,*]

[1]Department of Neurology and Neurological Sciences, Stanford University School of Medicine, Stanford, CA 94305

[2]Department of Neuroscience, Tufts University School of Medicine, Boston, MA, 02111, USA

[3]Graduate Program in Neuroscience, Stanford University School of Medicine, Stanford, CA 94305

[4]Neurology Service, Veterans Affairs Palo Alto Health Care System, Palo Alto, CA 94304

Summary

Biochemical studies suggest that excitatory neurons are metabolically coupled with astrocytes to generate glutamate for release. However, the extent to which glutamatergic neurotransmission depends on this process remains controversial, as direct electrophysiological evidence is lacking. The distance between cell bodies and axon terminals predicts that glutamine-glutamate cycle is synaptically localized. Hence we investigated isolated nerve terminals in brain slices by transecting hippocampal Schaffer collaterals and cortical Layer-I axons. Stimulating with alternating periods of high frequency (20Hz) and rest (0.2Hz), we identified an activity dependent reduction in synaptic efficacy that correlated with reduced glutamate release. This was enhanced by inhibition of astrocytic glutamine synthetase and reversed or prevented by exogenous glutamine. Importantly, this activity dependence was also revealed with an *in vivo* derived natural stimulus both at network and cellular levels. These data provide direct electrophysiological evidence that an astrocyte-dependent glutamate-glutamine cycle is required to maintain active neurotransmission at excitatory terminals.

Introduction

Synaptic transmission requires a continuous supply of neurotransmitter for release. While most types of neurons use direct reuptake to recycle released neurotransmitters, evidence indicates that glutamatergic synapses rely predominantly on astrocytes for generation and recycling of glutamate (Hertz, 1979). Biochemical studies demonstrate that astrocytes take up glutamate and convert it to glutamine, which is released into extracellular space and

*To whom correspondence should be addressed at hirotaniwork@gmail.com, rjreimer@stanford.edu.

taken up by neurons as a glutamate precursor in what is known as the glutamate-glutamine cycle. The cycle is generated by a segregated expression pattern for key molecular components. Astrocytes express high affinity excitatory amino acid transporters that clear released glutamate from the synapse, along with glutamine synthetase that converts glutamate to glutamine, and transporters that release glutamine into the extracellular space. In a reciprocal fashion, neurons express transporters that mediate uptake of glutamine, phosphate activated glutaminase that converts glutamine back to glutamate, and the machinery necessary for packaging and releasing glutamate through vesicle exocytosis (Danbolt, 2001). This model of cellular cooperation and compartmentalization predicts that efficacy at glutamatergic synapses is coupled to both astrocytic and neuronal metabolism. However, attempts to define a role for the glutamate-glutamine cycle in regulating excitatory synaptic transmission with standard electrophysiological analysis have met with limited success (Kam and Nicoll, 2007; Masson et al., 2006). In fact, a requirement for the cycle has only been demonstrated during epileptiform activity, a disease setting in which glutamate release is greatly increased (Bacci et al., 2002; Otsuki et al., 2005; Tani et al., 2010).

Studies in living animals have demonstrated that ~70% of synaptic glutamate is derived from the glutamate-glutamine cycle (Kvamme, 1998; Lieth et al., 2001; Rothman et al., 2003; Sibson et al., 2001). How can these *in vivo* studies be reconciled with electrophysiological analyses of isolated brain slices that suggest that glutamatergic neurotransmission can be sustained in the absence of the glutamate-glutamine cycle (Kam and Nicoll, 2007; Masson et al., 2006)? We reasoned that the lack of direct evidence for its requirement reflects the absence of an appropriate system in which to test this. For excitatory neurons with long axonal projections, the physical distance between the neuronal cell body and the presynaptic terminal limits the contribution of somatic sources to the pool of glutamate available for synaptic release (Kam and Nicoll, 2007; Masson et al., 2006). This suggests that a peri-synaptic localization of the glutamate-glutamine cycle would be required for maintaining high frequency neurotransmitter release from these neurons. We therefore investigated glutamate release from isolated nerve terminals by taking advantage of the anatomy of two well defined projection neuron tracts in the hippocampus and the cortex. By acutely transecting the axons we separated excitatory nerve terminals from their cell bodies while retaining the relationship of presynaptic structures with post-synaptic neurons and surrounding astrocytes. We found that these isolated terminals provide a reliable system for electrophysiological analysis of the role of the glutamate-glutamine cycle in excitatory neurotransmission. During moderate activity we found that glutamate release could be sustained in the absence of the glutamate-glutamine cycle, but not indefinitely, suggesting that there is a reservoir of glutamate and/or glutamine. Using a stimulation paradigm with alternating periods of robust activity and rest, we identified an activity dependent reduction in synaptic efficacy that correlated with a reduction in glutamate release. The reduced efficacy was greater with inhibition of astrocytic glutamine synthetase and fully reversed or prevented by addition of glutamine. Surprisingly, the rate of recovery did not differ in untransected slices, suggesting that in an intact brain a local glutamate-glutamine cycle is the predominant pathway for excitatory neurotransmitter recycling. Further, natural stimulation patterns derived from *in vivo* recordings resulted in a similar glutamine responsive activity dependent reduction in synaptic efficacy. This was observed at

the level of individual synapses with minimal stimulation while recording intracellularly from CA1 neurons. Together these findings demonstrate a role for a synaptically localized glutamate-glutamine cycle in maintaining excitatory neurotransmitter synthesis and vesicle release during periods of robust activity.

Results

To study the role of the glutamate-glutamine cycle in the release of neurotransmitter from axotomized terminals, we first focused on the Schaffer collateral pathway in the hippocampus. Synapses of the Schaffer collateral pathway are among the most extensively studied in the mammalian brain and the well-delineated structure of the hippocampus permits simple isolation of the presynaptic Schaffer collateral axons from their CA3 cell bodies while retaining the structural relationship of the presynaptic bouton with the post synaptic structures and perisynaptic astrocytes. Furthermore, bursts of 20–30 Hz activity lasting more than a minute have been observed in the mouse hippocampus during novel environment exploration (Berke et al., 2008). Thus, Schaffer collateral fibers release and must recycle or synthesize large amounts of glutamate to sustain such activities. Studies *in vitro* have also demonstrated that stimulation of Schaffer collateral fibers at 20 Hz drives excitatory neurotransmission at a maximal rate and exhausts the readily releasable pool of vesicles in ~3 sec (Dobrunz and Stevens, 1997; Garcia-Perez et al., 2008; Stevens and Wesseling, 1999; Wesseling and Lo, 2002). Beyond this time point, a steady state of vesicle recycling is established and the rate of neurotransmitter replenishment can define the sustained rate of release. With addition of N-methyl-D-aspartate (NMDA) receptor antagonists to block long-lasting plasticity, this experimental system allows for a direct electrophysiological analysis of the role of neurotransmitter synthesis in excitatory neurotransmission.

In hippocampal slices with Schaffer collateral fibers transected and perfused with standard artificial cerebro-spinal fluid (aCSF), we established a stable baseline of evoked field excitatory post-synaptic potentials (fEPSPs) in the stratum radiatum with 0.2 Hz stimulation. A baseline was typically obtained within 10–15 min and the fEPSPs remained stable for more than 60 min (Figure 1a, left panel). To test whether the capacity to release glutamate for extended periods of time depends upon the glutamate-glutamine cycle, we pre-incubated slices with methionine sulfoximine (MSO), an irreversible inhibitor of the astrocytic enzyme glutamine synthetase (GS). GS is required for both the glutamate-glutamine cycle and synthesis of glutamine derived *de novo* through anaplerosis (Schousboe et al., 1993). With a stimulation frequency of 0.2 Hz the fEPSPs in the MSO pretreated slices remained stable for 60 min (Figure 1a, right panel), consistent with previous findings (Kam and Nicoll, 2007; Masson et al., 2006). However, with the stimulation frequency increased to 2 Hz, after about 1000 stimuli there was a progressive reduction in fEPSP amplitudes in MSO treated slices (Figure 1b, black trace). To confirm that this effect was due to inhibition of GS, we added 500 μM glutamate, a concentration in the physiological range (Moore et al., 1978). This mitigated the effect of MSO (Figure 1b, green trace and right panels), indicating that there is a reservoir of glutamate and/or metabolic precursors that can sustain activity during prolonged periods of low frequency activity, but can be depleted by periods of more robust activity.

The experiments with MSO treated slices indicated that that the glutamate-glutamine cycle is necessary for sustained excitatory neurotransmission during prolonged periods of activity. We wondered whether the demand on an intact glutamate-glutamine cycle might be exceeded by its capacity during robust activity. Assaying slices not treated with MSO and increasing the stimulation rate to 20 Hz, we found the fEPSP amplitudes initially increased and then rapidly decreased to the point of being nearly undetectable (Figure 1c, black tracing). If this was due to loss of glutamate and/or its metabolic precursor glutamine in the effluate, then supplementation with glutamine should attenuate the loss of synaptic transmission. With addition of 500 μM glutamine, the initial increases and decreases in fEPSP amplitudes were similar to those in control slices during the first ~1000 pulses (50 sec), but after that the relative fEPSPs amplitudes were greater than those in control slices and remained stable for the duration of the experiment (Figure 1c green tracing). This indicates that, in the presence of glutamine, synaptic transmission at isolated Schaffer collateral terminals can be maintained during prolonged periods of high frequency stimulation.

The rapid decline in post-synaptic responses seen with 20 Hz stimulation in the presence of glutamine likely reflects high-frequency induced short-term synaptic depression caused by a limited availability of release-ready vesicles (Dobrunz and Stevens, 1997; Sara et al., 2002; Stevens and Wesseling, 1999). We reasoned that a pattern of high frequency stimulation alternating with periods of low frequency stimulation might allow readily releasable vesicle pools to be replenished without necessarily allowing neurotransmitter levels to recover fully. This could lead to more neurotransmitter release over time and place a greater demand on glutamate supply sources. Therefore we used a stimulation protocol interleaving high frequency stimuli (HFS; 20 Hz) for 50 sec (1000 pulses) with low frequency stimuli (LFS; 0.2 Hz) for 200 sec (40 pulses) hereafter referred to as intermittent high frequency stimulation (iHFS) protocol. We chose 50 sec for the HFS interval both because this is the point at which we started to see an effect with glutamine in the continuous HFS paradigm and because this is within the range of physiological bursts of high frequency activity in the hippocampus (Berke et al., 2008). With the iHFS protocol, we are also able to analyze synaptic activity during the periods of LFS, without confounding factors associated with high frequency stimulation such as changes in releasable vesicle pool size (Dobrunz and Stevens, 1997; Sara et al., 2002; Stevens and Wesseling, 1999). With iHFS we again found a decrease in the evoked fEPSP amplitudes during 20 Hz stimulation, but also a further progressive decrease with subsequent HFS iterations (Figure 2a, left panel). When slices were treated with glutamine there was also a decrease in the fEPSP amplitudes during 20 Hz stimulation train, but full recovery between HFS iterations (Figure 2a, right panel). The time course of fEPSPs demonstrates a robust cumulative glutamine-sensitive reduction in fEPSPs with iHFS that persisted for more than 5 min after termination of the final 20 Hz iteration (Figure 2b left panel upper tracings and right panel). In the glutamine treated slices the fEPSPs rapidly recovered to baseline at 0.2 Hz after HFS. This suggests that that vesicle pools are replenished quickly during LFS and that in the absence of glutamine the incomplete recovery was due to depletion of glutamate available for neurotransmission. Interestingly, the reduction in fEPSP amplitudes with iHFS and subsequent recovery during low frequency stimulation were similar in transected and intact hippocampal slices (Figure

S1). The fEPSP amplitudes remained reduced by more than half in both groups even 5 min after iHFS was completed.

While we suspected that limited neurotransmitter supply was the primary cause for the reduced fEPSPs after prolonged high frequency activity, another possible explanation was that the efficacy with which electrical stimulation elicited an action potential waned. To determine whether this contributed to the reduced synaptic signaling, we examined fiber volleys (FV) during the periods of 0.2 Hz stimulation. Aside from transient suppression during HFS, FVs were stable over the course of the experiment, and were not affected by glutamine (Figure 2b left panel lower tracings, Figure S2), indicating that there were no long-term changes in intrinsic excitability of the stimulated fibers by iHFS or by glutamine.

We next sought to ensure that the glutamine responsive reduction in fEPSP amplitude did not reflect diffuse metabolic changes in the slice. To assess this we compared input-output (I-O) curves from two laterally displaced stimulating electrodes, with one site stimulated as above with the iHFS protocol and the other (control) assessed continuously at 0.2 Hz, while recording from a single central recording electrode. With the iHFS protocol there was a significant depression (rightward shift) of the I-O curve, especially for small to moderate fiber volley amplitudes. This shift was not noted for the control electrode (Figure 2c left panel) or for either electrode with slices incubated with glutamine (Figure 2c right panel), suggesting that the effects of iHFS and glutamine are limited to the synapses that have been activated.

To determine how long this effect of high frequency activity on synaptic efficacy would last, we monitored fEPSPs during an extended recovery period. We found that after the iHFS protocol in aCSF, there was a slow recovery of fEPSP amplitudes that was still incomplete after 20 min (Figures 3a and 3b). With subsequent addition of glutamine, the recovery of fEPSP amplitude appeared to be hastened and near complete within 20 min. We next compared recovery during an extended LFS period after completion of iHFS without and with glutamine. Without glutamine there was little increase in the average relative fEPSP amplitude between 30 and 60 min after iHFS (0.53 +/− 0.30 and 0.59 +/− 0.29 respectively; p=0.239 paired two tailed t-test). There was, however, a significant recovery when glutamine was added at the start of the extended LFS period (0.58 +/− 0.22 and 0.82 +/− 0.34 respectively; p=0.0128 paired two tailed t-test). The addition of glutamine did not affect the FV, but caused normalization of the I-O curve (Figure 3c), consistent with its specific effect on the stimulated pathway.

The extent to which endogenous glutamine synthesized by astrocytes is required for the sustained periods of high frequency excitatory synaptic transmission in our system is unclear, but the reduction in synaptic efficacy caused by the gliotoxins fluoroacetate and fluorocitrate suggests that astrocytes are required for maintenance of excitatory neurotransmission (Bacci et al., 2002; Bonansco et al., 2011; Keyser and Pellmar, 1994). To test this we pre-incubated slices with MSO to inhibit the astrocytic enzyme glutamine synthetase. We expected that MSO would cause a more rapid reduction in fEPSP amplitude and that this effect would be attenuated by the addition of glutamine. We found that pretreatment of slices with MSO had little effect on the evoked fEPSP amplitudes during the

first epoch of 20 Hz stimulation in the iHFS protocol, but with subsequent iterations the recovery between HFS trains was much less complete than in untreated slices – ultimately fEPSPs were abolished (Figure 4a left panel). Even after 20 min of LFS the fEPSP amplitudes did not recover in the MSO treated slices (Figure 4b). With addition of glutamine to the MSO treated slices there was complete and persistent recovery between iterations of the high frequency stimulation and no discernable difference between MSO treated slices rescued with glutamine and slices to which glutamine alone was added (*cf.* Figure 4a right panel to Figure 2a right panel). Further, when glutamine was added to MSO treated slices after iHFS, there was a complete recovery of fEPSP amplitudes and normalization of I-O curves, again with no discernable difference with slices to which glutamine was added (*cf.* Figures 4b and 4c to Figures 2b and 2c). The effect of MSO and its reversal with glutamine support the hypothesis that astrocyte derived glutamine is required for maintaining synaptic transmission during prolonged periods of intermittent high frequency activity.

Reductions in synaptic efficacy can occur through a number of different mechanisms including changes in post-synaptic responsiveness (Collingridge et al., 2010). To confirm that our results reflect changes in glutamate release we used two independent approaches. First, we used FRET-based glutamate biosensor imaging to measure extracellular glutamate transients (Figure 5a). This biosensor is a chimeric protein composed of cyan fluorescent protein (CFP) and the yellow fluorescent protein (YFP) variant Venus inserted into the N-terminal and C-terminal regions of the bacterial glutamate binding protein YbeJ respectively. Glutamate binding causes a conformational change in the protein that results in a decrease in FRET efficiency between the CFP and Venus. The biosensor allows for qualitative measurement of glutamate release in brain slices throughout an optic field with temporal resolution in the millisecond scale (Dulla et al., 2008; Dulla et al., 2012). As expected, we found a decrease in glutamate biosensor signal with evoked release following HFS and this was prevented by glutamine (Figure 5b). As a second approach we used the competitive AMPA receptor antagonist gamma-D-glutamylglycine (γ-DGG) to assess synaptic glutamate levels (Christie and Jahr, 2006; Liu et al., 1999). This low-affinity antagonist has rapid equilibration kinetics with AMPA receptors and competes with glutamate for receptor binding during the glutamate transient associated with exocytosis. As a result, lower concentrations of glutamate are more effectively blocked by γ-DGG. We found that the effect of γ-DGG was enhanced even after only two iterations of HFS (Figure 5c). In slices pretreated with MSO, the effect of γ-DGG was again enhanced by iHFS, while with addition of glutamine to MSO pretreated slices, the efficacy of γ-DGG was unchanged by iHFS (Figure 5d and 5e). Together the findings with the biosensor and γ-DGG support the conclusion that iHFS leads to a reduction in glutamate release and reduced synaptic concentrations of glutamate.

Although unfilled synaptic vesicles can undergo exocytosis, it has been suggested that presynaptic cytosolic transmitter content influences vesicle release in cholinergic (Poulain et al., 1986) and GABAergic neurons (Wang et al., 2013). Since the paired pulse ratio depends upon the probability of release (Branco and Staras, 2009; Hanse and Gustafsson, 2001) we examined this after iHFS on MSO pretreated slices with and without glutamine. We found

an increase in paired pulse ratio after iHFS that was prevented by addition of glutamine, suggesting that glutamine influences release probability at excitatory synapses (Figure S3).

We wondered whether the dependence on the glutamate-glutamine cycle is shared by other excitatory synapses. To test this we established a system for electrophysiological analysis of neurotransmitter release from isolated Layer I axons in the neocortex (Figure 6a) based on a previously described preparation (Cauller and Connors, 1994). This allowed us to stimulate the axotomized fibers in Layer I and record synaptic responses from Layer III where the pyramidal cells are connected via distal apical dendrites projecting to layer I. At 0.2 Hz stimulation frequency we saw no reduction in the fEPSP amplitude (Figure 6b). We therefore again used the iHFS stimulation paradigm. Compared to the hippocampus, the neocortex was more resistant to the reduction in fEPSPs amplitude, requiring up to 13 iterations with 20 Hz stimulation to see a substantial loss of measurable fEPSPs. As with the hippocampal preparation, the reduction in fEPSP amplitude was eliminated by addition of glutamine to the perfusate (Figure 6c) and enhanced by pre-treatment with MSO (Figure 6d).

To determine whether dependence of excitatory neurotransmission on the glutamate-glutamine cycle can be elicited with naturally occurring neuronal activity, we obtained *in vivo* unit recordings representing firing patterns of single CA3 pyramidal cells from a freely-moving rat running laps in a field (courtesy of Dr. Kenji Mizuseki, Allen Institute for Brain Science and Dr. György Buzsaki, New York University Neuroscience Institute). We converted 12 minutes of continuous recording from two representative CA3 cells with low activity (natural low frequency stimulation; nLFS: mean 0.3 Hz, peak 6 Hz) and high activity (natural high frequency stimulation; nHFS: mean 5.4 Hz, peak 44 Hz) to time stamped stimulus patterns to drive the stimulators simultaneously on parallel Schaffer collateral fibers. This duration was chosen because it represented approximately 4000 pulses for nHFS (4032), consistent with other experiments. To obtain a baseline and assess recovery, fEPSPs were evoked at 0.2 Hz before and after the natural stimulus patterns. nHFS caused almost the same extent of fEPSP rundown as 4 iterations of iHFS, whereas there was no effect with nLFS (Figures 7a, b). Same slice comparisons were made by applying the natural stimulus patterns first in aCSF then with glutamine added. We found a glutamine responsive depression of fEPSP with nHFS, but not with nLFS (Figures 7b and 7c, top panel). Furthermore, amplitudes of fEPSPs 10 min after nHFS (Figure 7c, bottom panel) remained depressed in aCSF (0.478+/−0.079), but almost completely recovered in glutamine (0.975+/−0.084).

Finally, we evaluated the effects of neurotransmitter depletion at the synaptic level by repeating the experiments with natural stimulus patterns using minimal stimulation of Schaffer collateral fibers coupled with intracellular recordings of CA1 cells to more closely approximate *in vivo* CA3 neuronal activity. As with the field recordings, we established a baseline with 0.2 Hz stimulation at both electrodes, followed by 12 min during which one electrode was stimulated with the nLFS pattern and the other with the nHFS pattern. This was followed by a return to 0.2 Hz stimulation at both electrodes. Analysis of evoked EPSCs demonstrates that while there was no difference in evoked amplitudes after nLFS in aCSF or glutamine (Figures 8a and 8b), there was a significant reduction in minimally-evoked

amplitudes after nHFS in aCSF, but not in glutamine (Figures 8c and 8d). The reduction in EPSC amplitudes with nHFS in aCSF persisted for at least 10 min, consistent with our field recording results.

Discussion

The glutamate-glutamine cycle is a well established biochemical pathway, but direct evidence for its role in synthesis of synaptically released glutamate has been lacking. Indeed, results of previous physiological studies have argued against a requirement for the cycle in excitatory neurotransmission (Kam and Nicoll, 2007; Masson et al., 2006). Similar to these previous studies we found that with a low frequency stimulation protocol, glutamatergic synaptic transmission can persist for extended periods of time in the absence of a functional glutamate-glutamine cycle even from axotomized synaptic terminals. However, we found that increasing the stimulation frequency readily uncovered a requirement for the glutamate-glutamine cycle and that with both alternating periods of high frequency and low frequency stimulation and high frequency natural stimulus pattern the requirement was more apparent.

Our findings with the axotomized preparations indicate that prolonged high frequency excitatory neurotransmission can be sustained by a local synaptic glutamate-glutamine cycle. This model of a peri-synaptic intercellular metabolic pathway is supported by the subcellular expression of the molecular components of the cycle. End feet of astrocytes that surround synapses express the high affinity glutamate transporters as well as the System N glutamine transporters that are involved in glutamine efflux, while phosphate activated glutaminase that converts glutamine to glutamate is expressed in excitatory axons (Aoki et al., 1991; Boulland et al., 2002; Danbolt, 2001). Recently, coupling of glutamate uptake and glutamine release by astrocytes has been elegantly demonstrated (Uwechue et al., 2012). Billups and colleagues showed that uptake of glutamate released from neurons can trigger synthesis and release of glutamine from peri-synaptic astrocytes. Our findings provide direct evidence for the other half of the glutamate-glutamine cycle in neurotransmitter metabolism - *i.e.* utilization of glutamine by neurons for synthesis of synaptically released glutamate. Interestingly, Billups and colleagues detected glutamine release by measuring electrogenic glutamine uptake into the post-synaptic MNTB neuron at the Calyx of Held. As these neurons are GABAergic, their findings indicate that glutamine derived from synaptically released glutamate can serve as the precursor for the inhibitory neurotransmitter that modulates the excitatory network activity (Fricke et al., 2007; Liang et al., 2006).

The attenuation of rundown of fEPSPs by glutamine in both hippocampal Schaffer collateral and the neocortical Layer I preparations suggests that the local synaptic glutamate-glutamine cycle may be common to excitatory synapses of projection neurons throughout the mammalian central nervous system. The marked difference in rates of fEPSP depression in control conditions (*cf*. Figures 2b and 6c), despite the similar time course for fEPSP depression in MSO (*cf*. Figures 4b and 6d), suggests a regional variability in the glutamate-glutamine cycle. Interestingly, the number of synapses contacted by each astrocyte is four times higher in the hippocampus than in neocortex (Bushong et al., 2002; Halassa et al., 2007), indicating that the synapse/astrocyte ratio may define the capacity of the local glutamate-glutamine cycle and the capacity for sustained high frequency synaptic activity.

Our initial experiments, and those of others (Kam and Nicoll, 2007; Masson et al., 2006), suggest that synaptic transmission during LFS is completely independent of the cycle. Although the glutamate-glutamine cycle is the primary mechanism for recycling released glutamate (Bergles and Jahr, 1998), there is evidence for pre-synaptic uptake of glutamate and expression of the Na^+-dependent excitatory amino acid transporter GLT1 in Schaffer collaterals (Furness et al., 2008; Gundersen et al., 1993). However, the minimal recovery of fEPSPs of the MSO treated slices following iHFS suggests that the contribution from precursors other than glutamine and direct pre-synaptic glutamate reuptake cannot maintain the glutamate neurotransmitter pool even during periods of low frequency activity. A possible explanation for the absence of run down with LFS is that in the acutely isolated brain slice there is a large glutamate/glutamine reservoir that feeds into the neurotransmitter supply. This explanation is supported by our finding that the effect of MSO is only evident after 1000 stimuli at both 2Hz and 20 Hz stimulation.

If there is such a large supply of glutamate and glutamine available, is there any role for regulation of the glutamate-glutamine cycle in synaptic plasticity? Reduced synaptic efficacy associated with high frequency stimulation is a well-established phenomenon (Collingridge et al., 2010). The depletion of glutamate available for release that we describe may explain a portion of short-term synaptic depression associated with prolonged high frequency stimulation (Garcia-Perez et al., 2008; Stevens and Wesseling, 1999; Wesseling and Lo, 2002). Our iHFS paradigm likely creates a neurotransmitter supply demand similar to normal physiological phenomena including bursts of 20–30 Hz oscillations lasting many tens of seconds in the hippocampi of mice exploring novel environments (Berke et al., 2008; Hermann et al., 2007; Taberner and Liberman, 2005). Interestingly, compared to a continuous intense stimulus such as high potassium, intermittent high frequency activity likely leads to greater amounts of neurotransmitter release as the periods of low frequency activity allow for recovery of releasable vesicle pool that is rapidly depleted during intense stimulation (Sara et al., 2002). This may explain, in part, previous reports of sustained excitatory neurotransmission during intense stimulation (Kam and Nicoll, 2007; Masson et al., 2006). Further, the high frequency natural stimulus pattern led to a glutamine dependent rundown in synaptic efficacy that paralleled what we observed with iHFS. The mean firing frequency of nHFS pattern corresponds to the range of firing rates for place cells in field, whereas the nLFS that did not lead to a rundown in efficacy corresponds to the low end of activity of place cells in the field (Mizuseki and Buzsaki, 2013) and similar to the average firing rate of CA3 cells recorded during REM sleep (Mizuseki et al., 2012). The level of activity in our nHFS pattern is maintained *in vivo* much longer than replayed in our experiment and, as these recordings were from rodents running laps in a familiar environment without novel cues, the mean firing frequency in a novel environment may be even greater (Berke et al, 2008).

The mechanisms underlying the reduced synaptic efficacy with neurotransmitter depletion may involve both a reduction in release probability and a reduction in quantal size. The reduction in the amplitude of evoked responses with minimal stimulation after nHFS suggests a reduction in the amount of glutamate release with single synaptic events, consistent with previous findings of reduced synaptic event amplitudes with disruption of

the glutamate-glutamine cycle (Bonansco et al., 2011; Tani et al., 2010). Recent work has demonstrated that the recycling vesicle pool size and release probability at GABAergic synapses is reduced when cytosolic neurotransmitter supply is limited (Wang et al., 2013). This is consistent with previous studies of cholinergic synapses (Poulain et al., 1986) and with our findings of an increased paired pulse ratio in MSO treated slices after iHFS.

Although our data suggest that concentrations of glutamine in CSF provide a buffer, recent findings indicate that high frequency stimulation *in vivo* can reduce glutamine concentration at nerve terminals (Jenstad et al., 2009) suggesting that the capacity of the glutamate-glutamine cycle may provide a ceiling for the rate at which glutamate is released at excitatory synapses. The regulation of cycle components including System N transporters and glutamine synthetase may therefore provide a novel mechanism for altering synaptic efficacy in normal and diseased states (Balkrishna et al., 2010; Dai et al., 2012; Nissen-Meyer et al., 2011; Sidoryk-Wegrzynowicz et al., 2011).

Experimental Procedures

Preparation of brain slices

Briefly, following all guidelines of Stanford University's Institutional Animal Care and Use Committee, Sprague-Dawley rats (3–8 weeks) were anesthetized (55 mg/kg pentobarbital through intraperitoneal injection), decapitated, and the brains were rapidly removed and placed in chilled (4°C) low-Ca, low-Na^+ slicing solution consisting of (in mM): 234 sucrose, 11 glucose, 24 $NaHCO_3$, 2.5 KCl, 1.25 NaH_2PO_4, 10 $MgSO_4$ and 0.5 $CaCl_2$, equilibrated with a mixture of 95% O_2 and 5% CO_2. The brain was glued to the slicing stage of a Leica VT1200 sectioning system and slices (350 μm) were cut in a coronal orientation. The slices were then incubated for 1 h in 32°C oxygenated artificial cerebrospinal fluid (aCSF) consisting of (in mM): 126 NaCl, 26 $NaHCO_3$, 3 KCl, 1.25 NaH_2PO_4, 2 $MgCl_2$, 2 $CaCl_2$, and 10 glucose. For hippocampal slices, a transaction was made between CA1 and CA3 with a scalpel blade while the sectioned brain was in cold cutting solution.

Field recordings

Hippocampus—Slices were placed in an interface chamber maintained at 32–34°C and superfused with oxygenated aCSF at 2 mL/min and stimulated with a concentric bipolar electrode at Schaffer collaterals with 20–100 μA 100 μs pulses at 0.2 Hz (unless otherwise indicated) delivered by a stimulus isolator (World Precision Instruments, Sarasota, FL). Stimulus current was adjusted to induce FV amplitude of 0.15mV (+/−0.05mV) during the baseline period of the experiment, and was maintained at this level throughout the experiment except during I/O curve measurements. The I/O curve was normalized to the highest stimulus intensity tested (0.3 mV FV amplitude). For each slice two stimulating electrodes were placed on either sides of the recording electrode, with slight displacement to ensure stimulation of non-overlapping parallel Schaffer collateral pathways. Displacement position and stimulus sides were randomly altered between slices. During 0.2 Hz baseline data acquisition, the stimulation of the test (iHFS) pathway was interleaved with the stimulation of the control (no HFS) pathway 2.5 seconds apart.

Cortex—Slices were placed in an interface chamber with oxygenated aCSF and transected vertically from Layer II to the subcortical white matter and then horizontally below Layer I on one side of the vertical cut in aCSF with 10mM Mg. The slice was then superfused with oxygenated aCSF at 2ml/min with D-APV (50μM). The isolated Layer 1 fibers were stimulated with a concentric bipolar electrode with 20–100 μA 100 μsec pulses at 0.2 Hz, or as indicated.

aCSF contained 50 μM D-APV or 100 μM DL-APV with or without 500 μM glutamine as indicated. For MSO experiments, individual slices were incubated in freshly prepared 5 mM MSO in oxygenated aCSF for 1 hr at room temperature. We have previously shown that this treatment leads to a greater than 75% reduction in glutamine content in the slice (Tani et al, 2010). The slices were then transferred onto the recording rig in indicated aCSF solutions without MSO.

Electrophysiological data were recorded from glass micropipettes electrodes ~1 MΩ filled with aCSF using an Axon Multiclamp 700A amplifier and Digidata 1322A digitizer with pClamp software (Molecular Devices, Sunnyvale, CA). Slices with more than 40% change in FV amplitude during recording were discarded from analysis. Slices were also excluded from analysis if a spreading depression-like event, defined as a concurrent and significant unprovoked change in evoked fEPSPs from both stimulating electrodes, occurred.

Natural stimulus pattern

Twelve minutes of *in vivo* unit recordings from two CA3 pyramidal cells from an adult male Long-Evans rat running laps in a linear track field (as described in Mizuseki et al., 2009) were converted to time stamped stimulus patterns (100 μs per event), which was then played back as waveform patterns in 100 sec segments sequentially in Clampex to drive two stimulators simultaneously while recording from a single recording electrode. Predefined temporal patterns allowed discrimination of nLFS and nHFS post-analysis.

Whole cell recordings

Whole-cell voltage-clamp recordings were made from CA1 pyramidal cells using 2–5 MΩ pipettes filled with a solution containing (in mM): 120 K gluconate, 10 HEPES, 11 KCl, 1 $MgCl_2$, 11 EGTA, 1 $CaCl_2$ (pH 7.3). During EPSC recordings, the CA1 cell membrane were clamped at −57.7 mV and pharmacologically isolated AMPA currents were recorded by bath application of the GABAA receptor antagonist picrotoxin (50 μM, Tocris) and NMDA receptor antagonist (D-APV, 50 μM); access resistance was monitored at beginning and end of the recordings, and only cells with stable access resistance were included in the analysis. Stimulation setup was the same as for field potential recordings. A modified minimal stimulation approach based on (Dobrunz and Stevens, 1997) was used. Briefly, pulse pairs (40 msec interval) were applied at 0.2 Hz while adjusting stimulus strength to find conditions of minimal stimulation. The stimulus current was varied until a range of current was found for which three parameters were met: the EPSC amplitude remained constant, failures were observed, and a small reduction in stimulus amplitude resulted in 100% failures. Typically, this range was 10–50 pA.

For evoked EPSCs, a low pass Gaussian filter was used at 1k Hz to reduce signal to noise ratio and fitted the peak-to-baseline values for amplitudes over 2–3 ms range centered at the peak of the average current. Values smaller than 5 pA that were indistinguishable from noise were considered failures and were not included in the analysis of evoked EPSC amplitude. Failure rate was assessed and found to be unchanged in each condition (data not shown). Average raw amplitude values in each condition were not significantly different from one another, and ranged from 20–26 pA. Normality was assessed by performing Shapiro-Wilk Normality test and statistical significance by performing one-way ANOVA or Kruskal-Wallis one-way ANOVA on Ranks.

Biosensor imaging

Glutamate biosensor data were collected and analyzed as previously described (Dulla et al., 2008). Briefly, 50 µL of FLII81E–1 µM FRET-based glutamate biosensor protein (50 ng/µL) was applied to the slice on a 35 mm culture dish filled with 2 mL aCSF in a humidified chamber. After 10–20 min of incubation, the slice was placed into the recording chamber for simultaneous imaging and electrophysiological recording (Dulla et al., 2008). The slice was illuminated with 440 nm light and CFP (426–446 nm range) and Venus (505–565 nm range) signals were imaged at 500 Hz with a RedShirt Neuro-CCD camera. Ratiometric glutamate biosensor movies were collected during 10 successive stimulations and adjusted for bleaching using an exponential decay and then averaged. From the averaged movie an integrated glutamate response was generated by summing 30 frames of baseline subtracted data. The region of biosensor signal change was determined by threshold analysis. Briefly, all pixels with an integrated change in FRET <0.001 were discarded and the remaining pixels were ranked based on intensity. The pixels with the 90th–100th percentile most intense signal were selected and stray pixels were eliminated using an erosion filter. This region of interest was then used to analyze the FRET ratio for each individual glutamate movie and the response (FRET ratio) was averaged for all 10 movies. In order to generate representative images for each response the FRET images were blanked outside of the region of interest and overlaid on a brightfield image of the isotopic area.

Drugs and reagents

All salts and glucose for use in buffers were obtained from Sigma-Aldrich (St. Louis, MO). In addition the following reagents were also obtained from Sigma-Aldrich: L-methionine sulfoximine (MSO; M5379), L-glutamine (G3126). γ-DGG (ASC-307), D-APV (ASC-003) and DL-APV (ASC-004) were obtained from Ascent Scientific.

Data analysis

Data recorded by pClamp were analyzed using Clampfit software (Molecular Devices, Sunnyvale, CA), as well as with in-house software written in Matlab. Relative changes in fEPSP amplitudes and area were analyzed as indicated.

Statistics

Unless otherwise indicated, statistical significance for all experiments was determined using Student's unpaired and paired t-tests as well as ANOVA, as appropriate.

Supplementary Material

Refer to Web version on PubMed Central for supplementary material.

Acknowledgments

References

Aoki C, Kaneko T, Starr A, Pickel VM. Identification of mitochondrial and non-mitochondrial glutaminase within select neurons and glia of rat forebrain by electron microscopic immunocytochemistry. J Neurosci Res. 1991; 28:531–548. [PubMed: 1714509]

Bacci A, Sancini G, Verderio C, Armano S, Pravettoni E, Fesce R, Franceschetti S, Matteoli M. Block of glutamate-glutamine cycle between astrocytes and neurons inhibits epileptiform activity in hippocampus. J Neurophysiol. 2002; 88:2302–2310. [PubMed: 12424271]

Balkrishna S, Broer A, Kingsland A, Broer S. Rapid downregulation of the rat glutamine transporter SNAT3 by a caveolin-dependent trafficking mechanism in Xenopus laevis oocytes. Am J Physiol Cell Physiol. 2010; 299:C1047–1057. [PubMed: 20739622]

Bergles DE, Jahr CE. Glial contribution to glutamate uptake at Schaffer collateral-commissural synapses in the hippocampus. The Journal of neuroscience : the official journal of the Society for Neuroscience. 1998; 18:7709–7716. [PubMed: 9742141]

Berke JD, Hetrick V, Breck J, Greene RW. Transient 23–30 Hz oscillations in mouse hippocampus during exploration of novel environments. Hippocampus. 2008; 18:519–529. [PubMed: 18398852]

Bonansco C, Couve A, Perea G, Ferradas CA, Roncagliolo M, Fuenzalida M. Glutamate released spontaneously from astrocytes sets the threshold for synaptic plasticity. The European journal of neuroscience. 2011; 33:1483–1492. [PubMed: 21395864]

Boulland JL, Osen KK, Levy LM, Danbolt NC, Edwards RH, Storm-Mathisen J, Chaudhry FA. Cell-specific expression of the glutamine transporter SN1 suggests differences in dependence on the glutamine cycle. Eur J Neurosci. 2002; 15:1615–1631. [PubMed: 12059969]

Branco T, Staras K. The probability of neurotransmitter release: variability and feedback control at single synapses. Nature reviews Neuroscience. 2009; 10:373–383.

Bushong EA, Martone ME, Jones YZ, Ellisman MH. Protoplasmic astrocytes in CA1 stratum radiatum occupy separate anatomical domains. J Neurosci. 2002; 22:183–192. [PubMed: 11756501]

Cauller LJ, Connors BW. Synaptic physiology of horizontal afferents to layer I in slices of rat SI neocortex. J Neurosci. 1994; 14:751–762. [PubMed: 7905516]

Christie JM, Jahr CE. Multivesicular release at Schaffer collateral-CA1 hippocampal synapses. J Neurosci. 2006; 26:210–216. [PubMed: 16399689]

Collingridge GL, Peineau S, Howland JG, Wang YT. Long-term depression in the CNS. Nat Rev Neurosci. 2010; 11:459–473. [PubMed: 20559335]

Dai M, Xia XB, Xiong SQ. BDNF regulates GLAST and glutamine synthetase in mouse retinal Muller cells. J Cell Physiol. 2012; 227:596–603. [PubMed: 21448920]

Danbolt NC. Glutamate uptake. Prog Neurobiol. 2001; 65:1–105. [PubMed: 11369436]

Dobrunz LE, Stevens CF. Heterogeneity of release probability, facilitation, and depletion at central synapses. Neuron. 1997; 18:995–1008. [PubMed: 9208866]

Dulla C, Tani H, Okumoto S, Frommer WB, Reimer RJ, Huguenard JR. Imaging of glutamate in brain slices using FRET sensors. J Neurosci Methods. 2008; 168:306–319. [PubMed: 18160134]

Dulla CG, Tani H, Brill J, Reimer RJ, Huguenard JR. Glutamate biosensor imaging reveals dysregulation of glutamatergic pathways in a model of developmental cortical malformation. Neurobiol Dis. 2012; 49C:232–246. [PubMed: 22982711]

Fricke MN, Jones-Davis DM, Mathews GC. Glutamine uptake by System A transporters maintains neurotransmitter GABA synthesis and inhibitory synaptic transmission. J Neurochem. 2007; 102:1895–1904. [PubMed: 17504265]

Furness DN, Dehnes Y, Akhtar AQ, Rossi DJ, Hamann M, Grutle NJ, Gundersen V, Holmseth S, Lehre KP, Ullensvang K, et al. A quantitative assessment of glutamate uptake into hippocampal synaptic terminals and astrocytes: new insights into a neuronal role for excitatory amino acid transporter 2 (EAAT2). Neuroscience. 2008; 157:80–94. [PubMed: 18805467]

Garcia-Perez E, Lo DC, Wesseling JF. Kinetic isolation of a slowly recovering component of short-term depression during exhaustive use at excitatory hippocampal synapses. J Neurophysiol. 2008; 100:781–795. [PubMed: 18579659]

Gundersen V, Danbolt NC, Ottersen OP, Storm-Mathisen J. Demonstration of glutamate/aspartate uptake activity in nerve endings by use of antibodies recognizing exogenous D-aspartate. Neuroscience. 1993; 57:97–111. [PubMed: 7904057]

Halassa MM, Fellin T, Takano H, Dong JH, Haydon PG. Synaptic islands defined by the territory of a single astrocyte. J Neurosci. 2007; 27:6473–6477. [PubMed: 17567808]

Hanse E, Gustafsson B. Paired-pulse plasticity at the single release site level: an experimental and computational study. The Journal of neuroscience : the official journal of the Society for Neuroscience. 2001; 21:8362–8369. [PubMed: 11606624]

Hermann J, Pecka M, von Gersdorff H, Grothe B, Klug A. Synaptic transmission at the calyx of Held under in vivo like activity levels. J Neurophysiol. 2007; 98:807–820. [PubMed: 17507501]

Hertz L. Functional interactions between neurons and astrocytes I. Turnover and metabolism of putative amino acid transmitters. Prog Neurobiol. 1979; 13:277–323. [PubMed: 42117]

Jenstad M, Quazi AZ, Zilberter M, Haglerod C, Berghuis P, Saddique N, Goiny M, Buntup D, Davanger S, FM SH, et al. System A transporter SAT2 mediates replenishment of dendritic glutamate pools controlling retrograde signaling by glutamate. Cereb Cortex. 2009; 19:1092–1106. [PubMed: 18832333]

Kam K, Nicoll R. Excitatory synaptic transmission persists independently of the glutamate-glutamine cycle. J Neurosci. 2007; 27:9192–9200. [PubMed: 17715355]

Keyser DO, Pellmar TC. Synaptic transmission in the hippocampus: critical role for glial cells. Glia. 1994; 10:237–243. [PubMed: 7914511]

Kvamme E. Synthesis of glutamate and its regulation. Prog Brain Res. 1998; 116:73–85. [PubMed: 9932371]

Liang SL, Carlson GC, Coulter DA. Dynamic regulation of synaptic GABA release by the glutamate-glutamine cycle in hippocampal area CA1. J Neurosci. 2006; 26:8537–8548. [PubMed: 16914680]

Lieth E, LaNoue KF, Berkich DA, Xu B, Ratz M, Taylor C, Hutson SM. Nitrogen shuttling between neurons and glial cells during glutamate synthesis. J Neurochem. 2001; 76:1712–1723. [PubMed: 11259489]

Liu G, Choi S, Tsien RW. Variability of neurotransmitter concentration and nonsaturation of postsynaptic AMPA receptors at synapses in hippocampal cultures and slices. Neuron. 1999; 22:395–409. [PubMed: 10069344]

Masson J, Darmon M, Conjard A, Chuhma N, Ropert N, Thoby-Brisson M, Foutz AS, Parrot S, Miller GM, Jorisch R, et al. Mice lacking brain/kidney phosphate-activated glutaminase have impaired glutamatergic synaptic transmission, altered breathing, disorganized goal-directed behavior and die shortly after birth. J Neurosci. 2006; 26:4660–4671. [PubMed: 16641247]

Mizuseki K, Buzsaki G. Preconfigured, skewed distribution of firing rates in the hippocampus and entorhinal cortex. Cell Rep. 2013; 4:1010–1021. [PubMed: 23994479]

Mizuseki K, Royer S, Diba K, Buzsaki G. Activity dynamics and behavioral correlates of CA3 and CA1 hippocampal pyramidal neurons. Hippocampus. 2012; 22:1659–1680. [PubMed: 22367959]

Mizuseki K, Sirota A, Pastalkova E, Buzsaki G. Theta oscillations provide temporal windows for local circuit computation in the entorhinal-hippocampal loop. Neuron. 2009; 64:267–280. [PubMed: 19874793]

Moore JJ, Sax SM, Blackburn AB Jr. Determination of spinal fluid glutamine with the Du Pont aca. Clin Chem. 1978; 24:2213–2214. [PubMed: 719881]

Nissen-Meyer LS, Popescu MC, Hamdani el H, Chaudhry FA. Protein kinase C-mediated phosphorylation of a single serine residue on the rat glial glutamine transporter SN1 governs its membrane trafficking. J Neurosci. 2011; 31:6565–6575. [PubMed: 21525297]

Otsuki T, Nakama H, Kanamatsu T, Tsukada Y. Glutamate metabolism in epilepsy: 13C-magnetic resonance spectroscopy observation in the human brain. Neuroreport. 2005; 16:2057–2060. [PubMed: 16317354]

Parsons RL, Calupca MA, Merriam LA, Prior C. Empty synaptic vesicles recycle and undergo exocytosis at vesamicol-treated motor nerve terminals. Journal of neurophysiology. 1999; 81:2696–2700. [PubMed: 10368389]

Poulain B, Baux G, Tauc L. Presynaptic transmitter content controls the number of quanta released at a neuro-neuronal cholinergic synapse. Proceedings of the National Academy of Sciences of the United States of America. 1986; 83:170–173. [PubMed: 3510429]

Rothman DL, Behar KL, Hyder F, Shulman RG. In vivo NMR studies of the glutamate neurotransmitter flux and neuroenergetics: implications for brain function. Annu Rev Physiol. 2003; 65:401–427. [PubMed: 12524459]

Sara Y, Mozhayeva MG, Liu X, Kavalali ET. Fast vesicle recycling supports neurotransmission during sustained stimulation at hippocampal synapses. J Neurosci. 2002; 22:1608–1617. [PubMed: 11880491]

Schousboe A, Westergaard N, Sonnewald U, Petersen SB, Huang R, Peng L, Hertz L. Glutamate and glutamine metabolism and compartmentation in astrocytes. Dev Neurosci. 1993; 15:359–366. [PubMed: 7805590]

Sibson NR, Mason GF, Shen J, Cline GW, Herskovits AZ, Wall JE, Behar KL, Rothman DL, Shulman RG. In vivo (13)C NMR measurement of neurotransmitter glutamate cycling, anaplerosis and TCA cycle flux in rat brain during. J Neurochem. 2001; 76:975–989. [PubMed: 11181817]

Sidoryk-Wegrzynowicz M, Lee E, Mingwei N, Aschner M. Disruption of astrocytic glutamine turnover by manganese is mediated by the protein kinase C pathway. Glia. 2011; 59:1732–1743. [PubMed: 21812036]

Stevens CF, Wesseling JF. Identification of a novel process limiting the rate of synaptic vesicle cycling at hippocampal synapses. Neuron. 1999; 24:1017–1028. [PubMed: 10624963]

Taberner AM, Liberman MC. Response properties of single auditory nerve fibers in the mouse. J Neurophysiol. 2005; 93:557–569. [PubMed: 15456804]

Tani H, Dulla CG, Huguenard JR, Reimer RJ. Glutamine is required for persistent epileptiform activity in the disinhibited neocortical brain slice. J Neurosci. 2010; 30:1288–1300. [PubMed: 20107056]

Uwechue NM, Marx MC, Chevy Q, Billups B. Activation of glutamate transport evokes rapid glutamine release from perisynaptic astrocytes. J Physiol. 2012; 590:2317–2331. [PubMed: 22411007]

Wang L, Tu P, Bonet L, Aubrey KR, Supplisson S. Cytosolic transmitter concentration regulates vesicle cycling at hippocampal GABAergic terminals. Neuron. 2013; 80:143–158. [PubMed: 24094108]

Wesseling JF, Lo DC. Limit on the role of activity in controlling the release-ready supply of synaptic vesicles. J Neurosci. 2002; 22:9708–9720. [PubMed: 12427826]

Zhou Q, Petersen CC, Nicoll RA. Effects of reduced vesicular filling on synaptic transmission in rat hippocampal neurones. The Journal of physiology. 2000; 525(Pt 1):195–206. [PubMed: 10811737]

Highlights

- Direct electrophysiological evidence for glutamine glutamate cycle has been lacking

- Isolated nerve terminals show an activity dependent reduction in glutamate release

- Exogenous glutamine (500 μM) fully prevents and reverses activity-induced rundown

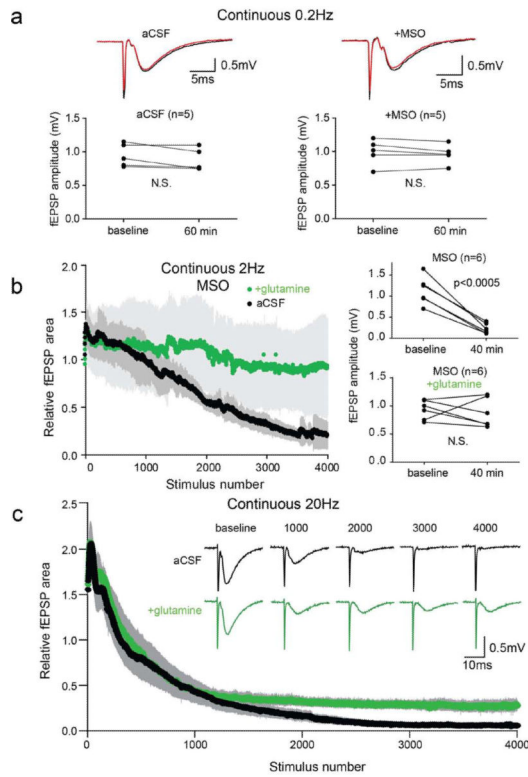- Astrocytic glutamine plays a crucial role in sustaining excitatory neurotransmission

Figure 1. Glutamine prevents fEPSP depression during high frequency repetitive stimulation of the Schaffer collaterals
(a) Example traces at baseline (black) and after 60 min (red) of continuous 0.2 Hz stimulation (upper) and paired plot of fEPSP amplitudes (lower) for untreated slices (left) and slices pretreated with MSO to inhibit glutamine synthetase (right). (b) Time course of relative fEPSP area during continuous 2 Hz stimulation (4000 stimuli; 33.3 min) of the Schaffer collaterals (left panel) in slices treated with MSO in aCSF (black; n=6) and with addition of 500 μM glutamine (green; n=6). Evoked fEPSP amplitudes during 0.2 Hz stimulation at baseline and at 40 min (~6 min after 2 Hz stimulation) shows significant fEPSP depression (Student's t-test, p<0.0005) in MSO treated slices but not in glutamine (right panel). (c) Time course of continuous 20 Hz stimulation of Schaffer collaterals in aCSF (black; n=6) and with glutamine (green, n=4). Inset: example traces at indicated stimulus numbers. Gray bars indicate SEM.
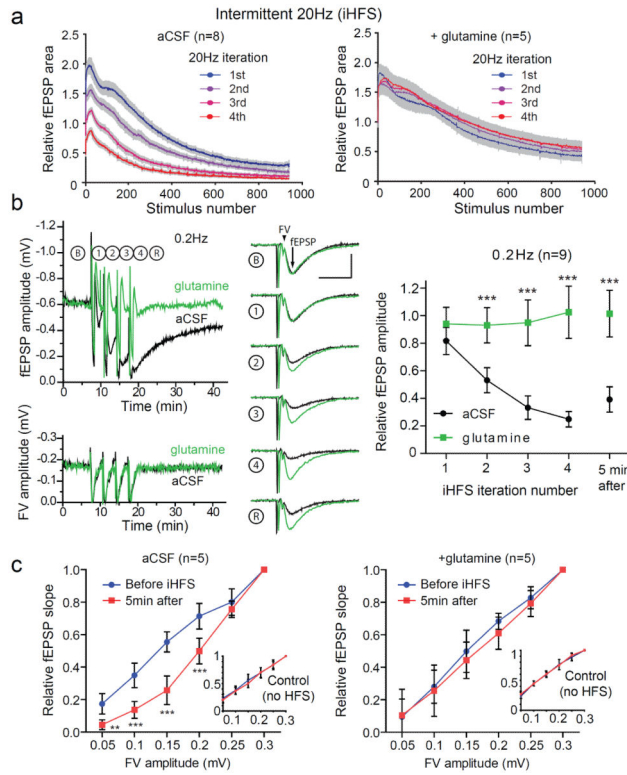
Figure 2. *iHFS* causes use-dependent fEPSP depression that is prevented by glutamine
(a) Evoked fEPSP amplitudes during intermittent 20 Hz stimulation with four iterations of 1000 pulses at 20 Hz separated by 200 sec of recovery at 0.2 Hz in aCSF (left panel; n=8) and aCSF with 500 μM glutamine (right panel; n=5). (b) Time course of fEPSP amplitude (upper left) and FV amplitude (lower left) during iHFS protocol on slices in aCSF (black) and aCSF with glutamine (green). Traces of evoked fEPSP during 0.2 Hz stimulation at baseline (B), after successive iterations of 1000 pulses at 20Hz (1–4), and after a subsequent 5 min recovery period (R) of 0.2Hz stimulation (middle panel) and summary (right panel; n=9, 2-way repeated measures ANOVA with Bonferroni post test, ***P<0.001, error bars represent 95% CI) demonstrate activity-dependent reduction in fEPSP amplitude. FV and fEPSP are indicated by the arrowhead and arrow respectively in baseline sample tracings in (b). Scale bars=10ms, 0.5mV. (c) Graphs of input (FV amplitude in mV) and output (relative fEPSP slope) are plotted for stimulated (iHFS) electrodes with control stimulation pathway (continuous 0.2 Hz stimulation) shown in insets. I/O curves before iHFS (blue) and after (red) in the absence (left) and presence (right) of glutamine (2-way repeated measures ANOVA with Bonferroni post test, **p<0.01, ***P<0.001, error bars represent 95% CI). The same recording electrode was used for iHFS and control stimulating electrodes.
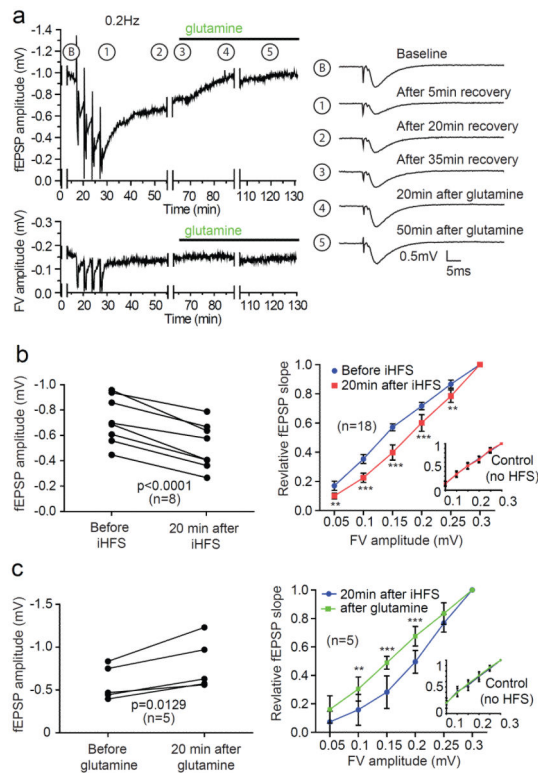
Figure 3. Glutamine reverses iHFS induced fEPSP amplitude reduction
(a) Time course of fEPSP amplitude (upper trace) and FV (lower trace) with standard iHFS protocol followed by addition of glutamine. Traces during collection of data for I/O relationship were removed (and depicted by gaps) for clarity. Example traces during 0.2 Hz stimulation at indicated time points are depicted on right. (b) Paired plot of fEPSP amplitude measurement before and after iHFS protocol (left panel) shows significant depression at 20 min after the iHFS (student's t-test, p<0.0001) and a corresponding rightward shift in the I/O curve (right panel). There is no change in the I/O curve for the control pathway (inset). (c) Addition of glutamine 20 min after iHFS protocol significantly increases fEPSP amplitude 20 min later (left panel; student's t-test, p=0.0129). There is also a corresponding leftward shift of the I/O curve (right panel). Note glutamine does not affect the I/O curve of the control pathway (inset). For statistical analyses of the I/O curves 2-way repeated measures ANOVA with Bonferroni post test was applied (**p<0.01, ***p<0.001).
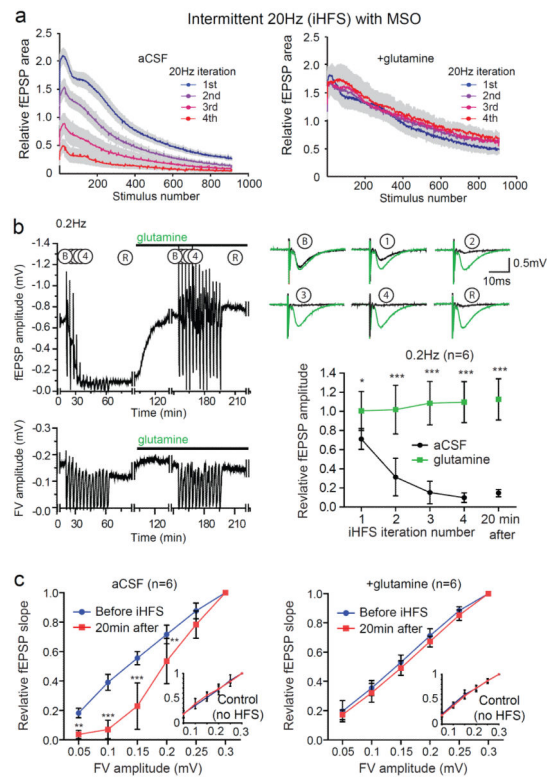
Figure 4. Inhibiting glutamine synthesis with MSO enhances iHFS induced fEPSP depression
(a) Evoked fEPSP amplitudes for MSO treated slices during four iterations of 1000 pulses at 20 Hz separated by 200 sec of recovery at 0.2 Hz in aCSF (left panel; n=8) and aCSF with 500 μM glutamine (right panel; n=5). (b) Representative time course of evoked fEPSPs (upper) and fiber volleys (lower) in MSO treated slice. Note that adding glutamine after iHFS was associated with recovery that persisted during an additional 13 HFS iterations. Gaps represent time periods during which data for the I/O relationship were being collected. Traces of evoked fEPSP during 0.2 Hz stimulation at baseline (B), after successive iterations of 1000 pulses at 20 Hz (1–4), and after a subsequent 5 min recovery period (R) of 0.2 Hz stimulation (upper right panel) and summary (lower right panel; n=6, 2-way repeated measures ANOVA with Bonferroni post test, *p<0.05, ***p<0.001, error bars represent 95% CI) demonstrate the reduction in fEPSP in the MSO treated slices and the recovery with addition of glutamine. (c) I/O curves before iHFS (blue) and after (red) for MSO treated slices in the absence (left) and presence (right) of glutamine (2-way repeated measures ANOVA with Bonferroni post test, **p<0.01, ***p<0.001, error bars represent 95% CI). Insets: I/O curves for laterally displaced control electrodes that were stimulated continuously at 0.2 Hz.
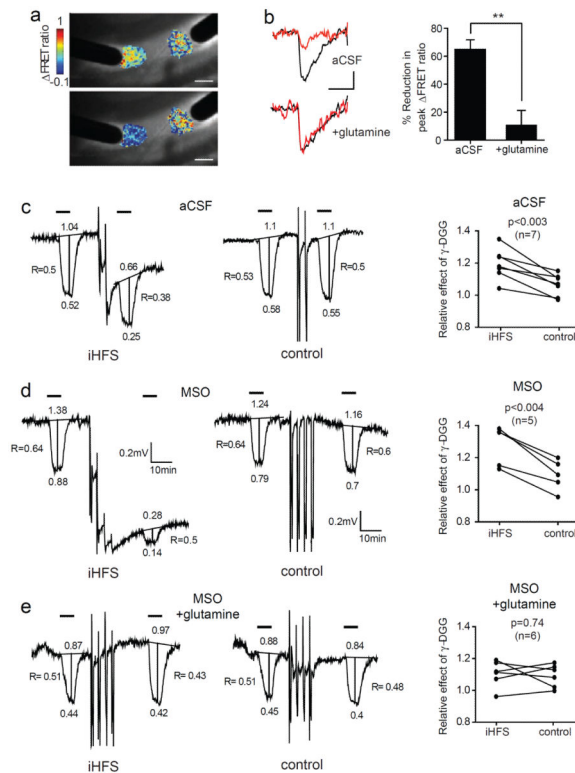
Figure 5. Reduction in evoked glutamate release after iHFS is prevented by addition of glutamine

(a) Representative heat maps of glutamate biosensor FRET change (FRET) for regions of interest adjacent to stimulating electrodes in the Schaffer collaterals overlayed on a bright-field image. Baseline signal (top panel) was obtained during an initial period of 0.2Hz stimulation at both electrodes. After the left electrode was subjected to iHFS protocol (bottom panel) there was a marked decrease in the signal, while there was little change in the signal at control electrode stimulated continuously at 0.2 Hz (right electrode). Scale bars=200μm. (b) Representative time course of evoked FRET signal change by iHFS stimulated electrode in aCSF (upper) and in glutamine (lower) at baseline (black) and after iHFS (red); scale bars=100ms, 0.005 FRET. Summary of the reduction in evoked peak FRET 5min after iHFS with and without glutamine (n=4 aCSF, n=7 glutamine, 1-way ANOVA, **p=0.002). There were no significant differences at the control electrode stimulated with continuous 0.2 Hz in presence and absence of glutamine (data not shown). (c–e) Effect of low-affinity, fast equilibrating AMPA receptor antagonist γ-DGG. Example traces and corresponding paired sample data (analyzed by student's t-test) showing the effect of 1 mM γ-DGG applied for 6 min (indicated as black bars in traces) before and after iHFS (left traces) compared to control electrode (right traces) in the same slice in (c) aCSF, (d) MSO pretreated slices, and (e) MSO pretreated slices to which glutamine was added. The bottom number represents the evoked amplitude 5min after addition of γ-DGG, and the top number represents the evoked amplitude in the absence of γ-DGG, derived from the evoked amplitudes immediately before and after γ-DGG wash-in. R is the ratio of the amplitude of γ-DGG effect to the baseline amplitude (equal to the bottom number divided by the top number). The change in effect of γ-DGG was calculated by determining the change in ratio of amplitude reduction caused by γ-DGG before and after iHFS.
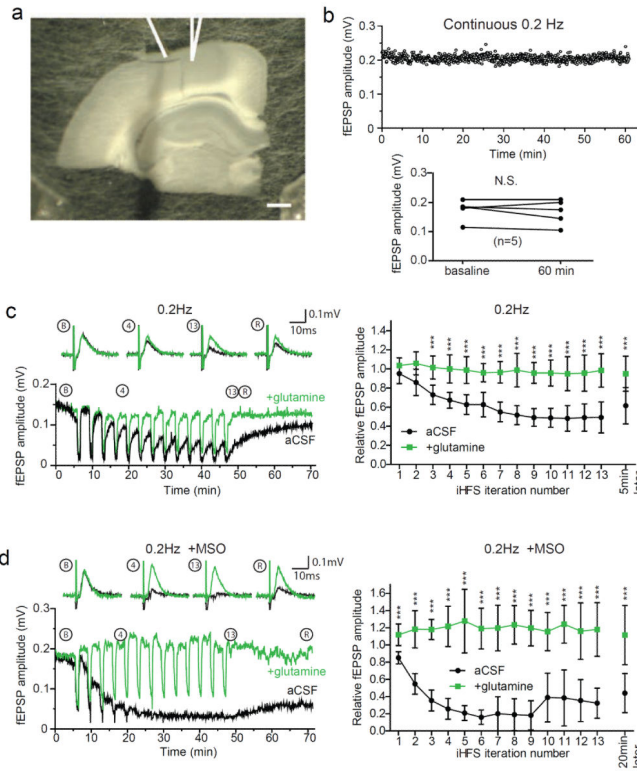
Figure 6. Glutamine prevents fEPSP depression during repetitive stimulation of Layer I cortical afferents
(a) Bright field image of rat brain slice in which Layer I cortical axons have been transected and separated from on column deeper layers. Positions of stimulating (left) and recording electrode (right; in Layer III where Layer V apical dendrites project) are depicted by line drawings. (b) Representative time course of evoked fEPSP amplitude during continuous 0.2Hz stimulation protocol (upper) and plot of paired fEPSP amplitude measurements at 5 min and 60 min for 5 slices stimulated continuously at 0.2 Hz (lower; student's t-test, no significant difference). (c) Representative time course of evoked fEPSP amplitudes recorded during 0.2 Hz stimulation period during baseline (B), after 4th (4) and 13th (13) HFS iteration, and during recovery (R) with sample traces above (black trace, aCSF; green trace, glutamine). Summary of fEPSP amplitude after each HFS iteration (right panel; n=5, 2-way repeated measures ANOVA with Bonferroni post test, ***p<0.001, error bars represent 95% CI). (d) As in (c) with slices preincubated with glutamine synthetase inhibitor MSO.
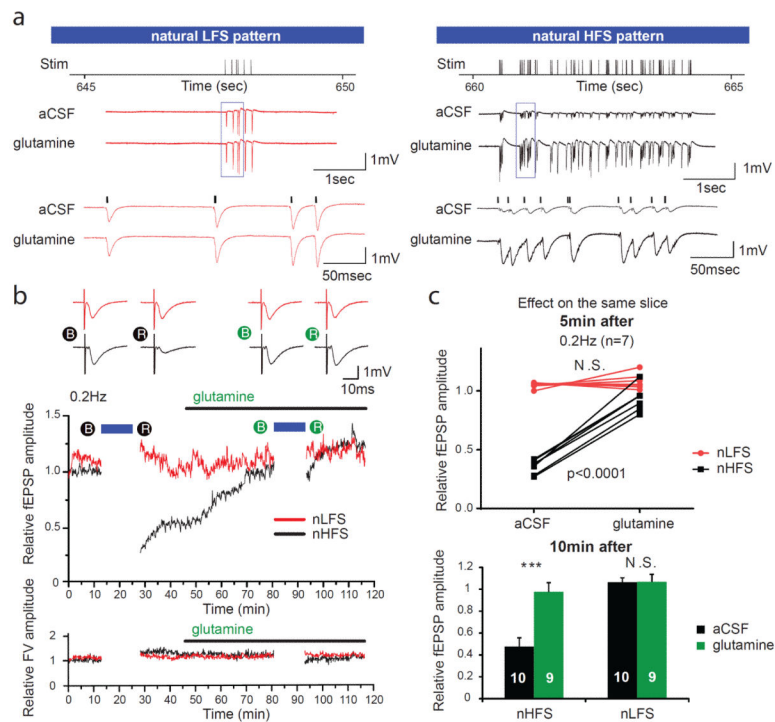
Figure 7. In vivo-derived natural stimulus pattern reveals glutamine-dependent reduction in evoked fEPSPs
Twelve minutes of *in vivo*-derived neuronal firing patterns were replayed as a natural low frequency stimulus (nLFS) or high frequency stimulus (nHFS) on parallel Schaffer collateral fibers in the absence or presence of glutamine. (a) Five seconds of representative field recording traces near the end of 12 min of nLFS and nHFS shows no difference between aCSF and glutamine treatment on the same slice with nLFS, but a significant depression in fEPSP amplitudes with nHFS that is prevented by glutamine. Stimulus artifacts were removed for clarity. (b) Traces of evoked fEPSPs (upper panel) during 0.2 Hz stimulation at baseline (B) and after 5 min recovery (R) from natural stimulus patterns for slices perfused first with aCSF (black filled circles, left) and then with aCSF plus glutamine (green filled circles, right). Traces of nLFS protocol electrode are in red and those of nHFS protocol electrode in black. Sample time course of relative fEPSP amplitude (middle panel) and FV amplitude (lower panel) evoked at 0.2 Hz during baseline acquisition and after recovery from nLFS (red) and nHFS (black) protocols initially in aCSF and then with addition of glutamine. Blue bars indicate duration of nLFS/nHFS. (c) Paired analysis of evoked fEPSP amplitudes in aCSF and aCSF with glutamine 5 min after natural stimulus protocols (top) revealed no difference in evoked fEPSP amplitudes after nLFS, but fEPSP amplitude depression with nHFS in aCSF that was markedly attenuated in the presence of glutamine (n=7, 2-way repeated measures ANOVA with Bonferroni post test, P<0.0001). Relative fEPSP amplitudes remained significantly depressed 10 min after nHFS in aCSF (0.478+/−0.079; student's t-test, ***p<0.0001), but almost completely recovered in the presence of glutamine (0.975+/−0.084).
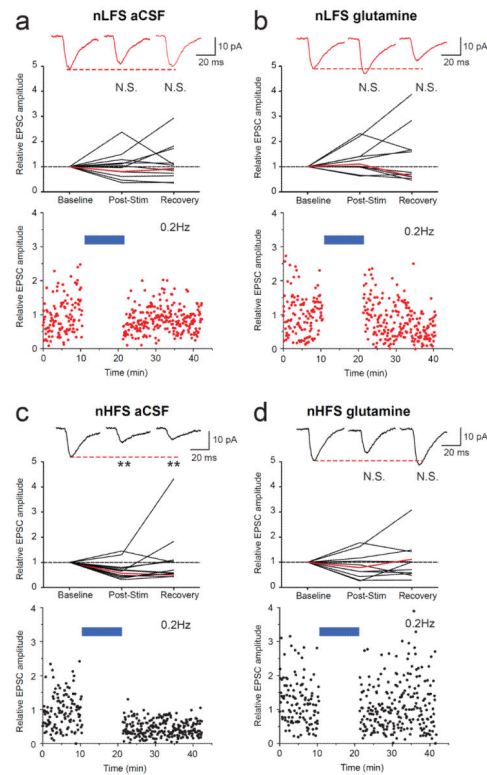
Figure 8. Minimally-evoked natural stimulus pattern reveals glutamine-dependent reduction in evoked synaptic EPSCs
EPSC amplitudes were analyzed from intracellular recordings of CA1 cells in which the Schaffer collaterals were minimally-stimulated with natural patterns in the absence or presence of glutamine. (a) Representative example of averaged minimally-evoked EPSC amplitudes (upper panel) during 0.2 Hz stimulation from a CA1 cell over 5 min during baseline (left), the first 5 min post-nLFS (middle) and 10–15 minutes post nLFS (right). Red dotted line represents mean baseline amplitude. Relative amplitudes of evoked EPSCs from 13 individual cells (middle panel) during baseline, the first 5 min post-nLFS (Post-Stim) and 10–15 minutes post nLFS (recovery). Red continuous line depicts representative median response corresponding to the representative traces. Time course of evoked EPSC amplitudes from a representative cell normalized to the median of the baseline (bottom panel). Blue bar represents duration of natural stimulus. (b–d) same as above but with (b) nLFS in glutamine (n=11), (c) nHFS in aCSF (n=13) and (d) nHFS in glutamine (n=11). A significant reduction of evoked EPSCs was seen with nHFS in aCSF during post-stim (0.65 median, **p<0.05) and recovery (0.58 median, **p<0.05), but not in glutamine (One way ANOVA; aCSF p=0.0134, glutamine p=0.9125 for difference within groups). There was no significant difference in evoked EPSCs with nLFS with or without glutamine.